Electronic Supplementary Information

In-situ Epitaxial Growth of Ag_3PO_4 Quantum Dots on Hematite Nanotubes for High Photocatalytic Activities

Junyuan Duan,[ab] Leilei Xu,[a] Youwen Liu[b], Bingxin Liu,[c] Tianyou Zhai*[b] and Jianguo Guan*[a]

a State Key Laboratory of Advanced Technology for Materials Synthesis and Processing, International School of Materials Science and Engineering, Wuhan University of Technology, Wuhan 430070, China. E-mail: guanjg@whut.edu.cn

b State Key Laboratory of Material Processing and Die & Mould Technology, School of Materials Science and Engineering, Huazhong University of Science and Technology, Wuhan 430074, China. E-mail: zhaity@hust.edu.cn

c Qinghai Provincial Key Laboratory of New Light Alloys, Qinghai University, Xining 810016, China

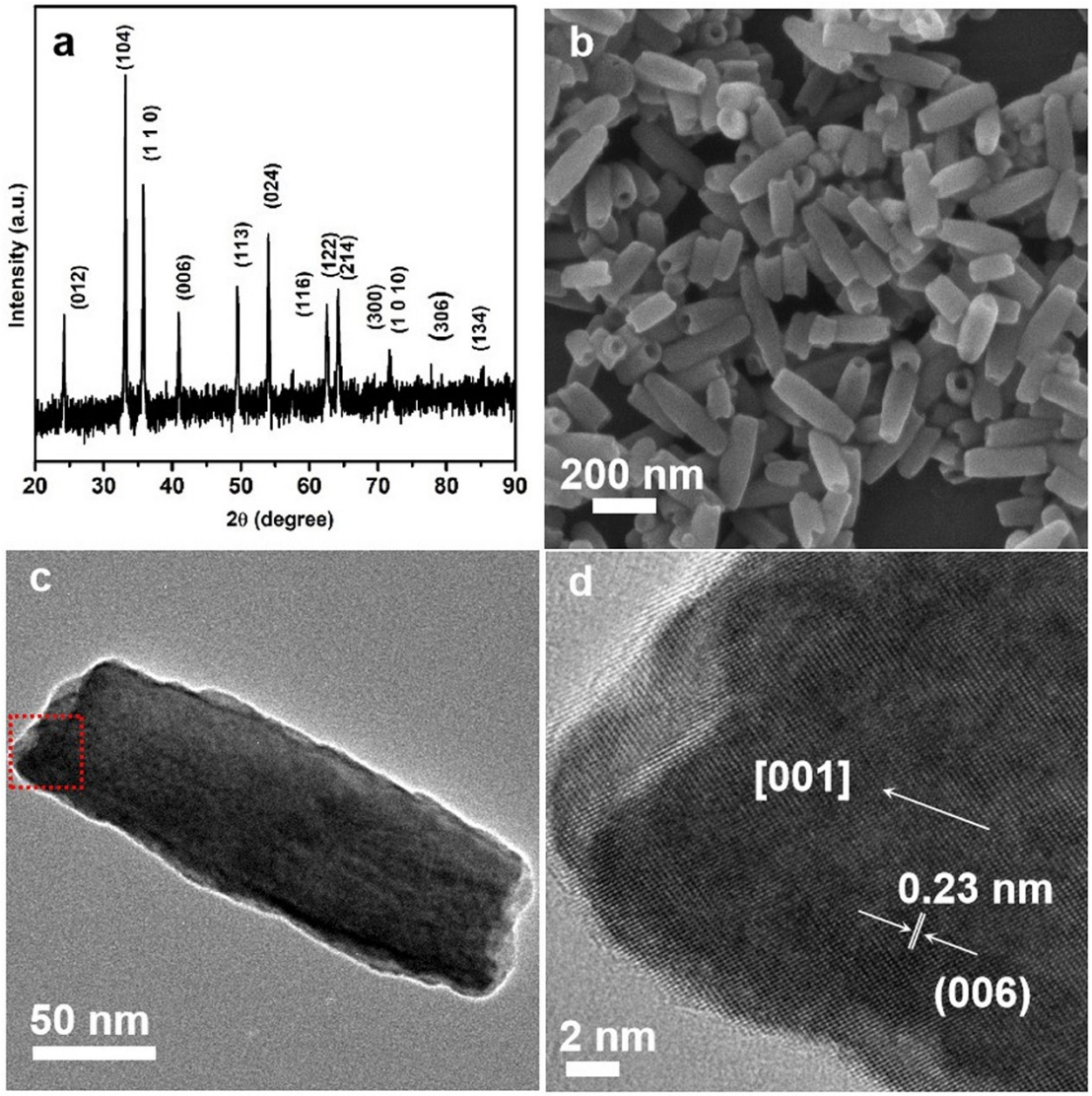

Fig. S1 (a) XRD pattern, (b) SEM and (c) TEM images of the Fe_2O_3 NTs; (e) the HRTEM image indicated with a rectangular frame in (c). The results indicate that the as-prepared products are uniform and dispersable hexagonal-phase Fe_2O_3 (JCPDS card No. 33-0664) single-crystalline NTs. They have a diameter of 60-80 nm and a length of 150-200 nm. The growth direction is along [001].

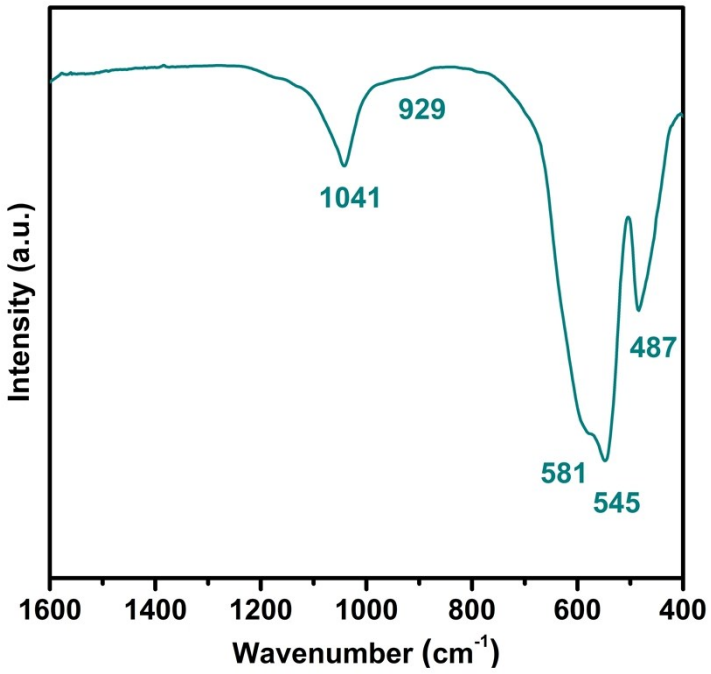

Fig. S2 FTIR spectrum of the pure Fe_2O_3 NTs. In the spectrum, the two absorption peaks at 1041 and 929 cm^{-1} correspond to the asymmetric stretching vibration of P-O-P group and symmetric stretching vibration of PO group of PO_4^{3-} anions, respectively. S1

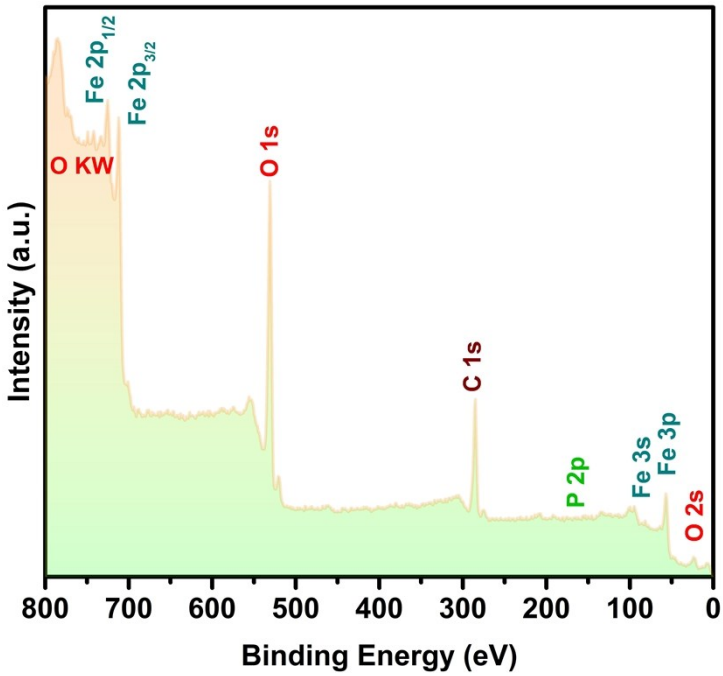

Fig. S3 XPS full spectrum of the pure Fe_2O_3 NTs.

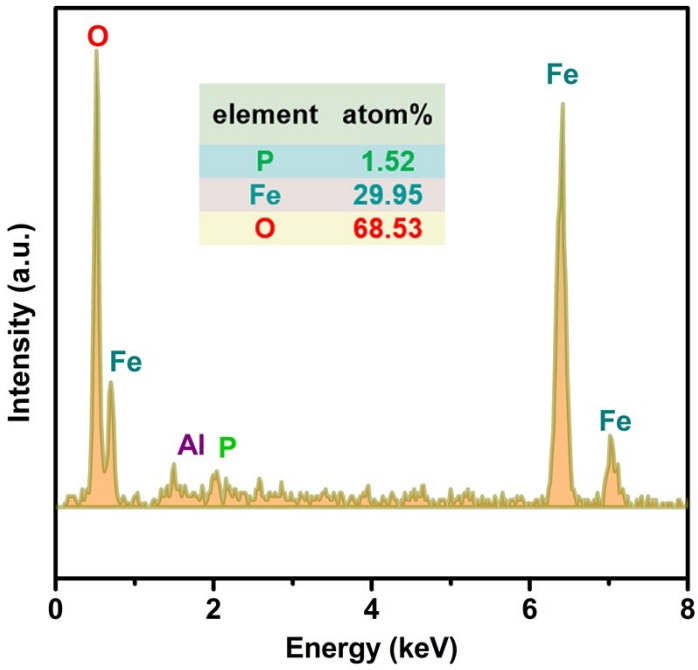

Fig. S4 EDX spectrum of the pure Fe_2O_3 NTs. The inset is the corresponding atomic ratio, indicating that the molar ratio of P to Fe in the Fe_2O_3 NTs is 0.05:1.

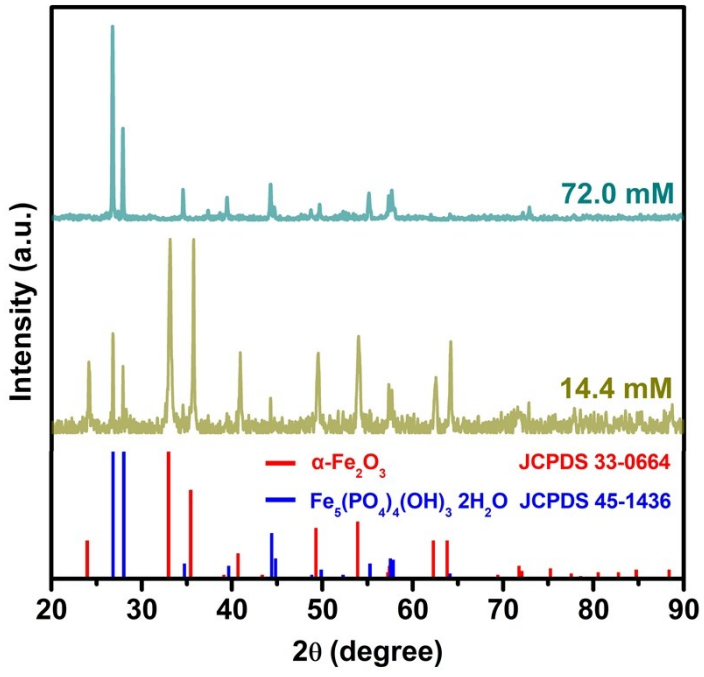

Fig. S5 XRD patterns of the samples obtained at [$NH_4H_2PO_4$] of 14.4 and 72.0 mM respectively, suggesting that the adsorbed phosphate anions in Fe_2O_3 NTs exist as a form of $Fe_5(PO_4)_4(OH)_3 \cdot 2H_2O$.

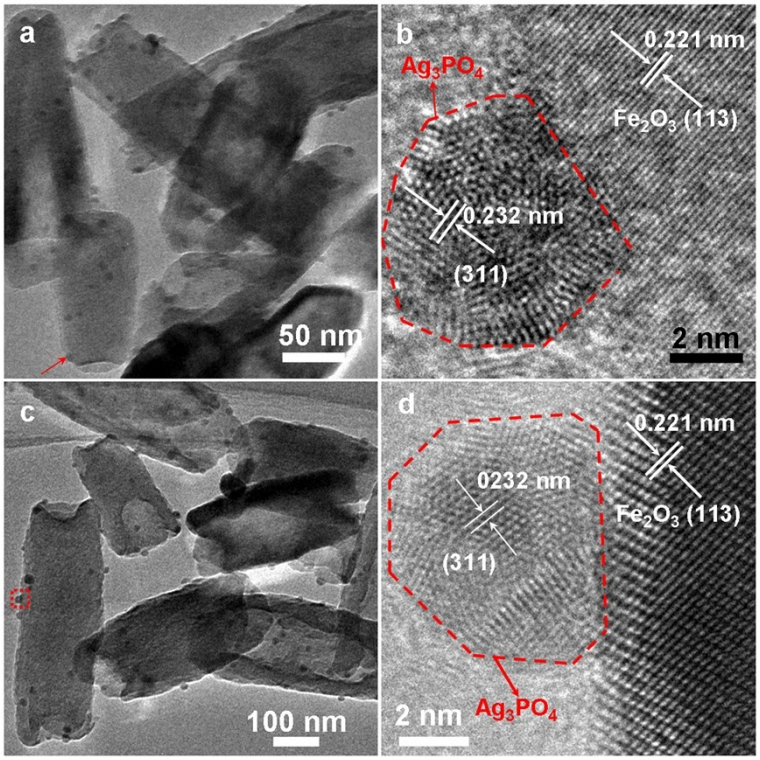

Fig. S6 (a, c) TEM images for two other junctions of Ag_3PO_4/Fe_2O_3 HNSs. (b, d) The corresponding HRTEM images of the areas indicated with an arrow and a rectangular frame in (a) and (c) respectively

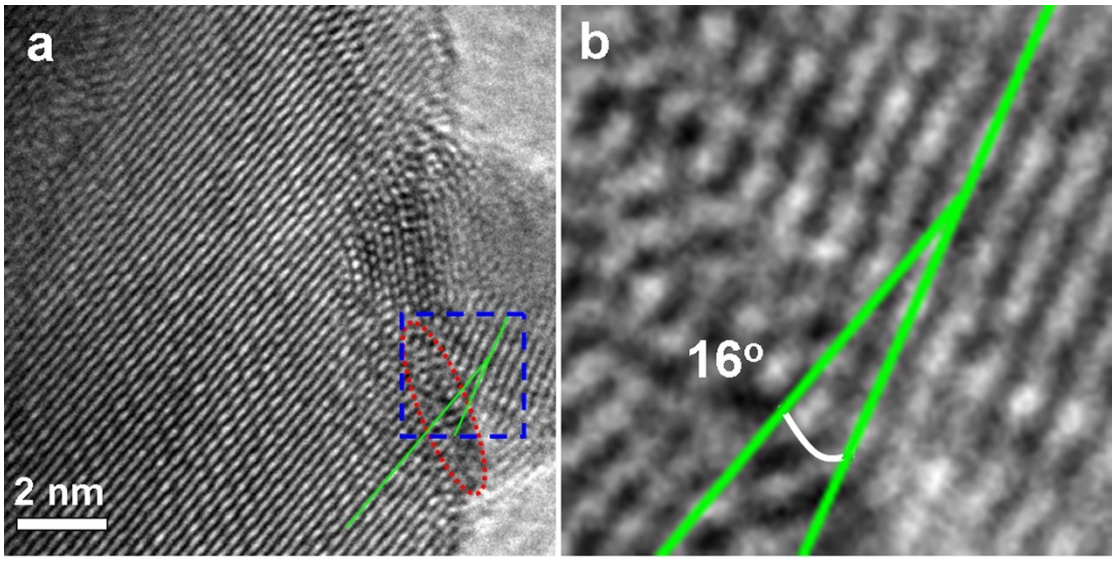

Fig. S7 (a) Constructed inverse FFT image along the growth direction for the HRTEM image of Figure 2c. (b) The enlarged image of the area indicated with a rectangular frame in (a). The area indicated by a red elliptical frame in (a) shows the typical lattice fringe distortion at the hetero-interface. The distortion at the hetero-interface was calculated to be 8.8% ((16°/180°)×100% = 8.8%). And the lattice mismatch between Ag_3PO_4 (311) and Fe_2O_3 (113) was 4.74% ((0.221-0.232)/0.232)×100% = 4.74%).

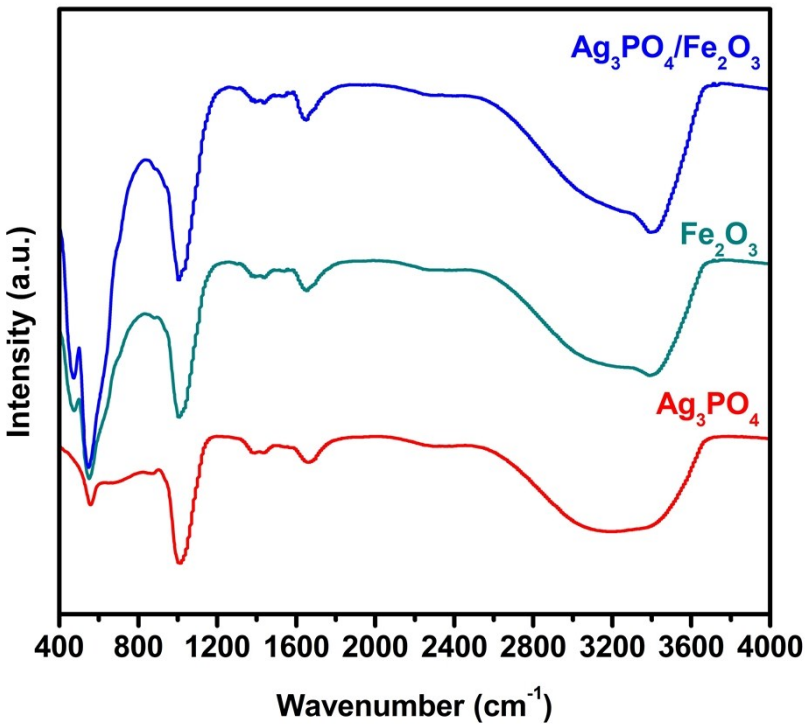

Fig. S8 FTIR spectra of the Fe_2O_3 NTs, Ag_3PO_4 and Ag_3PO_4/Fe_2O_3 NT-HNs.

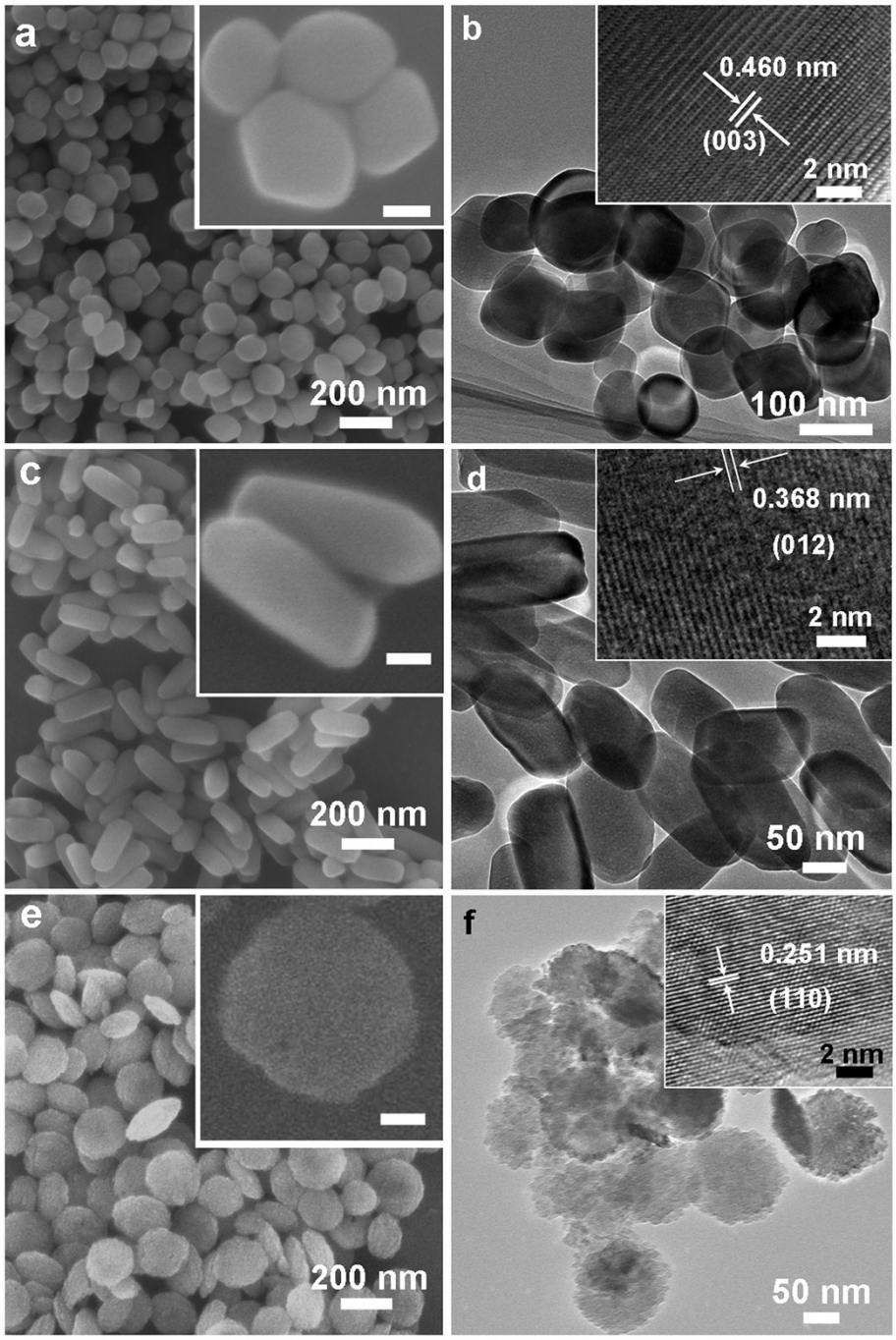

Fig. S9 SEM and TEM images of the Fe_2O_3 samples obtained at [$NH_4H_2PO_4$] of (a, b) 0, (c, d) 0.36 and (e, f) 1.44 mM respectively. The insets are the corresponding high magnification SEM (a, c and e) and HRTEM (b, d and f) images. The scale bars in the insets of (a), (c) and (e) are all 50 nm.

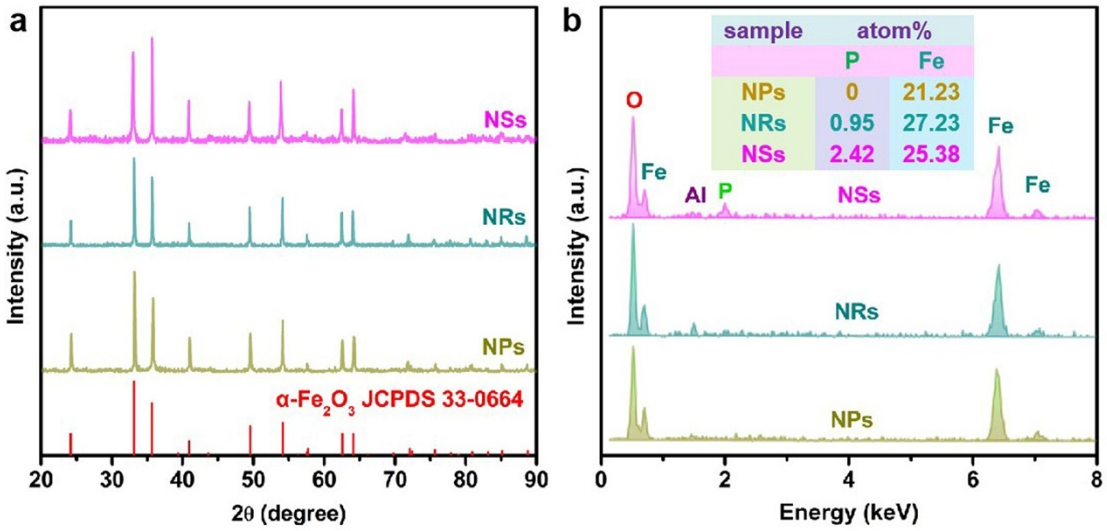

Fig. S10 (a) XRD patterns and (b) EDX spectra of Fe_2O_3 nanoparticles (NPs), nanorods (NRs) and nanosheets (NSs) samples. The inset in (b) lists the atomic percentage of P and Fe elements in the three samples, indicating that the atomic ratio of P to Fe in the Fe_2O_3 NPs, NRs and NSs is 0, 0.03:1 and 0.10:1, respectively.

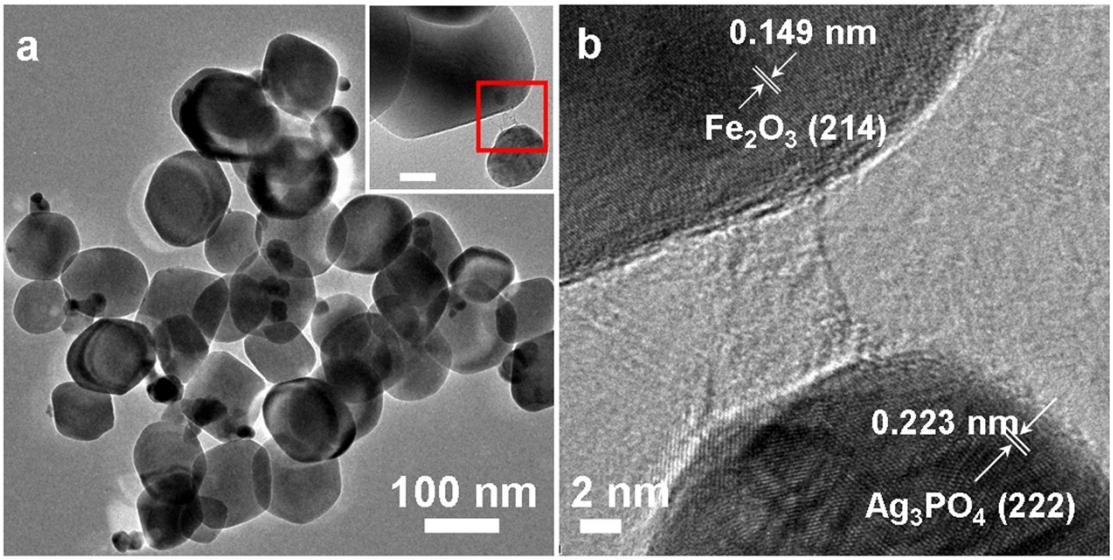

Fig. S11 TEM (a) and HRTEM (b) images of the samples obtained by using the Fe_2O_3 nanoparticles free of PO_4^{3-} as raw materials. The scale bar in the inset of (a) is 20 nm.

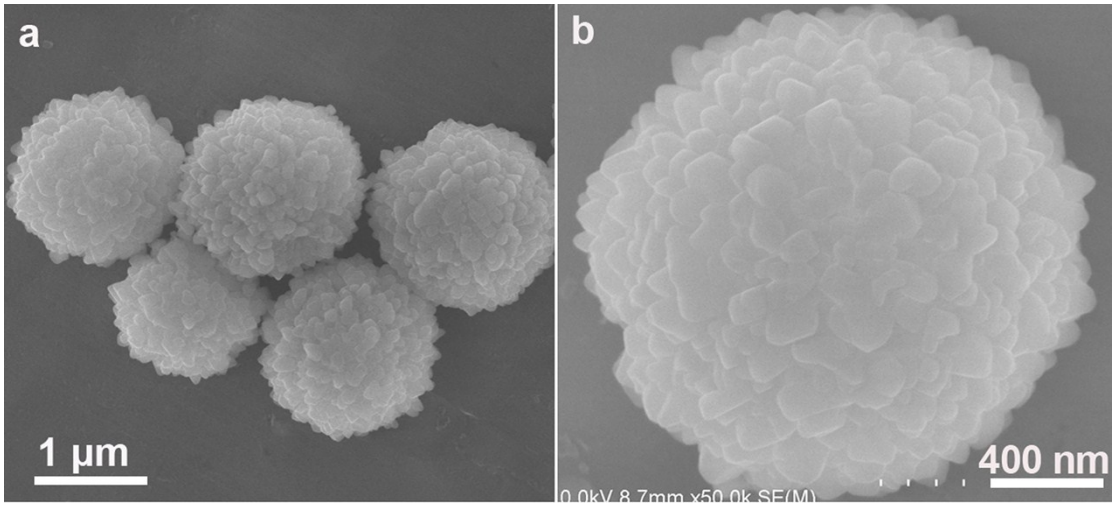

Fig. S12 (a, b) SEM images of the $Fe_5(PO_4)_4(OH)_3 \cdot 2H_2O$ particles corresponding to the samples obtained at $[NH_4H_2PO_4]$ of 72.0 mM.

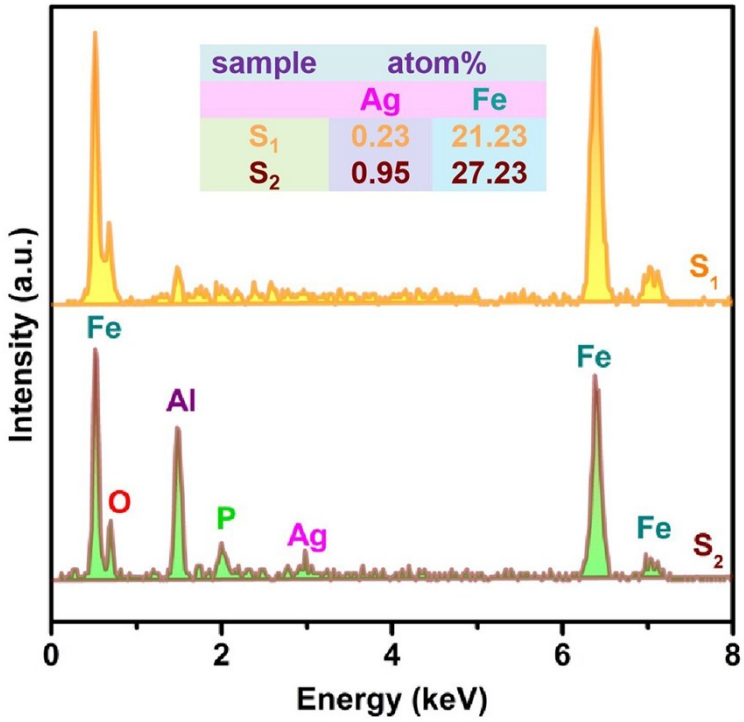

Fig. S13 EDX spectra of the Ag_3PO_4/Fe_2O_3 heterostructures obtained by using the Fe_2O_3 nanostructures with different PO_4^{3-} contents of 2.43% and 4.83% as raw materials.

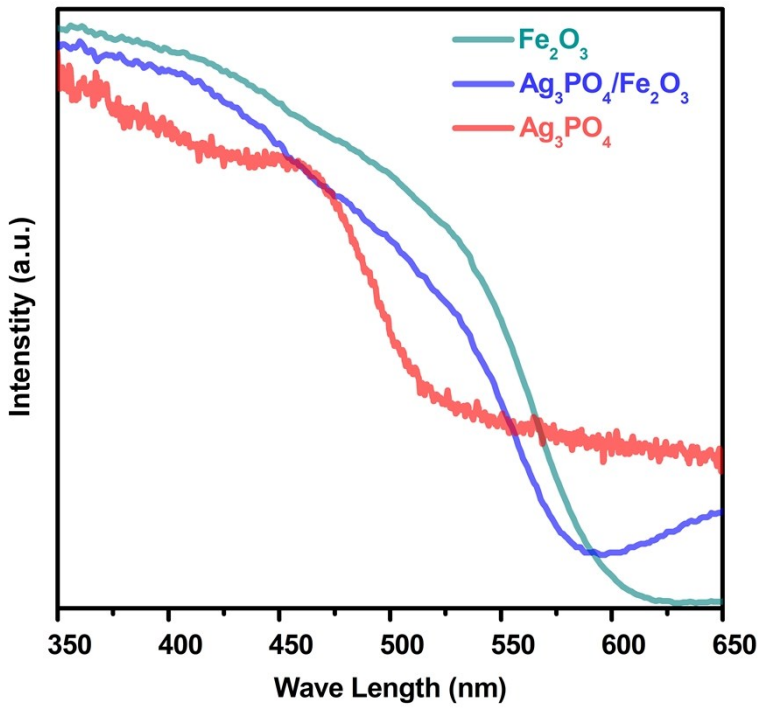

Fig. S14 UV/Vis absorption spectra of the as-prepared Ag_3PO_4/Fe_2O_3 NT-HNSs, Fe_2O_3 NTs and Ag_3PO_4 QDs.

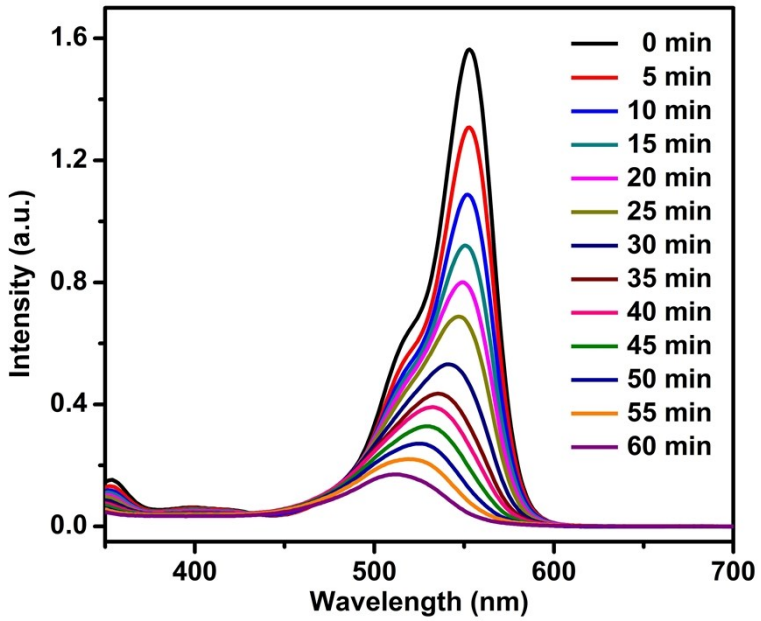

Fig. S15 Absorption spectra of the RhB solution containing the Ag_3PO_4/Fe_2O_3 NT-HNSs as a function of visible light irradiation time (*t*).

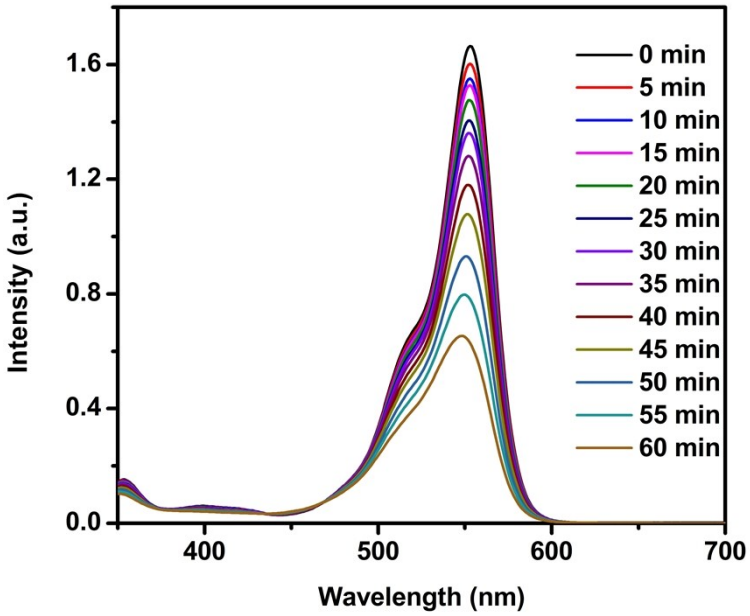

Fig. S16 Absorption spectra of the RhB solution containing the hetero-nanostructures photocatalysts with Ag_3PO_4 QDs growing on Fe_2O_3 NRs (Fig. 4 b-c) as a function of visible light irradiation time (*t*).

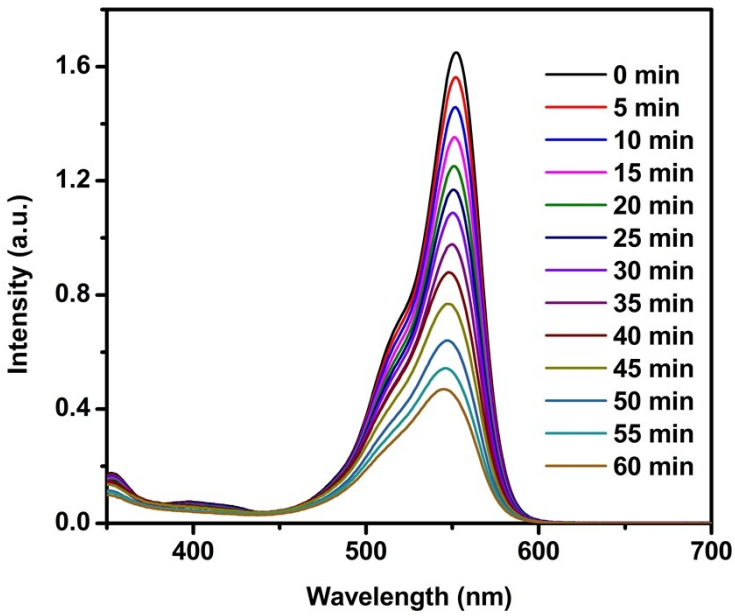

Fig. S17 Absorption spectra of the RhB solution containing the hetero-nanostructures photocatalysts with Ag_3PO_4 QDs growing on Fe_2O_3 NSs (Fig. 4 d-e) as a function of visible light irradiation time (*t*).

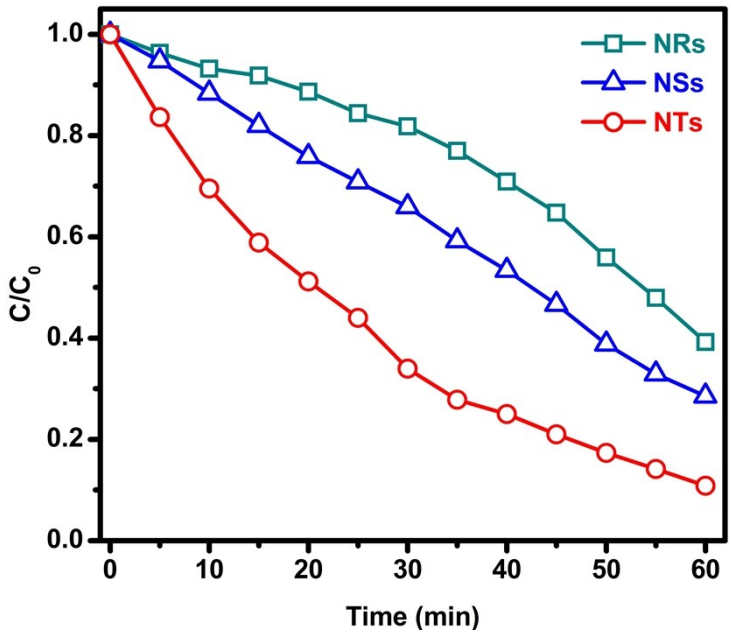

Fig. S18 Photocatalytic activities of the hetero-nanostructures photocatalysts with Ag_3PO_4 QDs growing on Fe_2O_3 NTs (Fig. 2), NRs (Fig. 4 b-c) and NSs (Fig. 4 d-e) for the decoloration of RhB in aqueous solution.

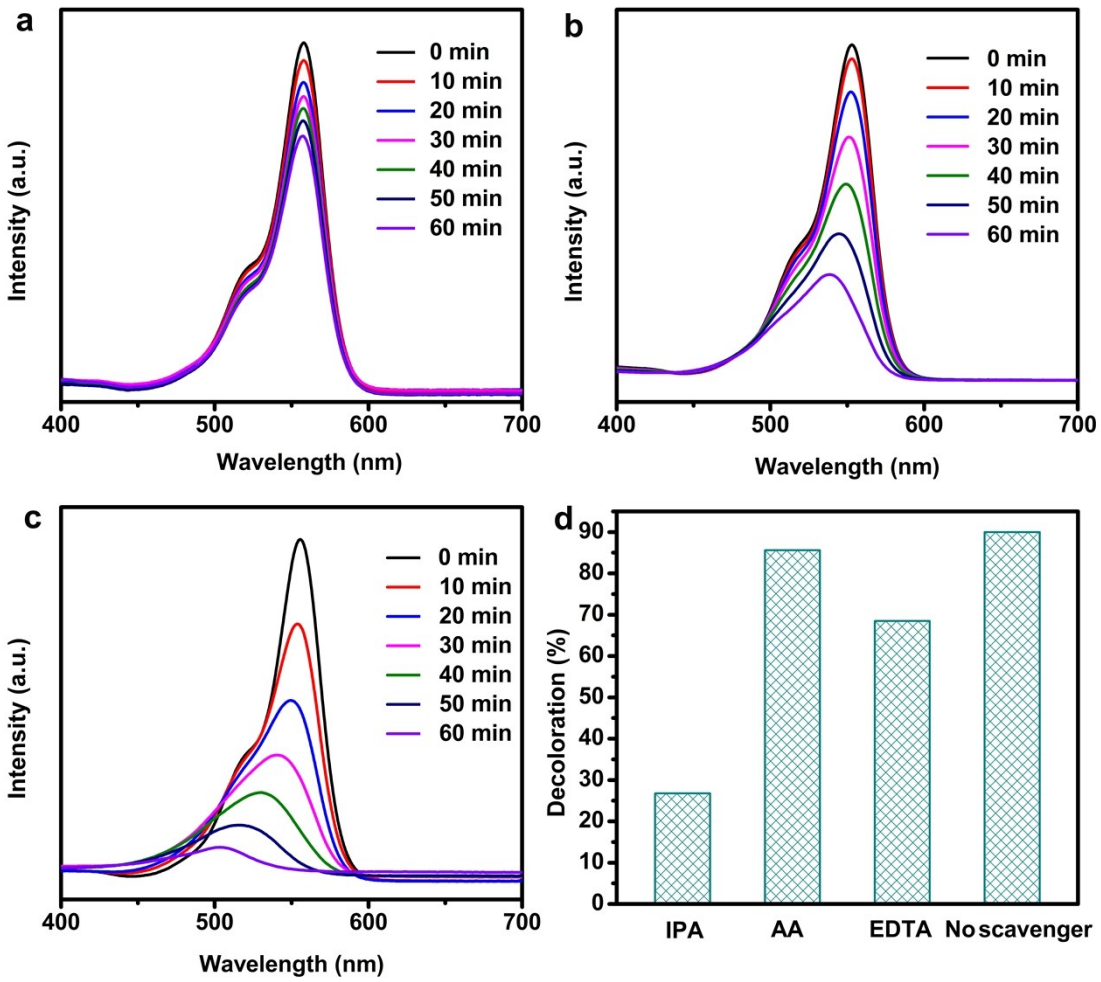

Fig. S19 Absorption spectra of the RhB solution over the Ag_3PO_4 /Fe_2O_3 NT-HNSs by using (a) IPA, (b) AA, (c) EDTA as scavenger respectively. (d) The decoloration rate of RhB over Ag_3PO_4/Fe_2O_3 HNSs with scavenger (IPA, AA, EDTA) or without scavenger.

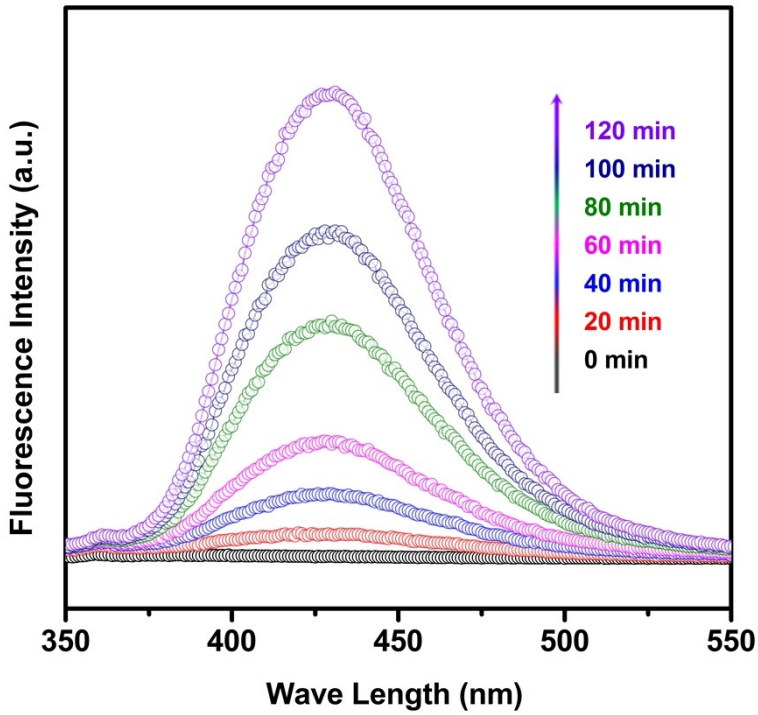

Fig. S20 PL intensity changes of the terephthalic acid at about 430 nm using Ag_3PO_4/Fe_2O_3 NT-HNSs as catalysts under light irradiation over time.

Reference

S1 C.J. Jia, L.D. Sun, Z.G. Yan, L.P. You, F. Luo, X.D. Han, Y.C. Pang, Z. Zhang and C.H. Yan, *Angew. Chem. Int. Ed.*, 2005, **44**, 4328-4333.